

# Long-range order coexisting with long-range entanglement: Is $\text{Nd}_2\text{Sn}_2\text{O}_7$ the first Coulombic antiferromagnet with a visible emergent gauge photon?

Gang Chen<sup>1,2\*</sup>

<sup>1</sup>The University of Hong Kong Shenzhen Institute of Research and Innovation, Shenzhen 518057, China and

<sup>2</sup>Department of Physics and HKU-UCAS Joint Institute for Theoretical and

Computational Physics at Hong Kong, The University of Hong Kong, Hong Kong, China

(Dated: August 18, 2022)

Exotic state of matter could coexist with conventional orders such that the gauge fields and fractionalized excitations could prevail in a seemingly ordered state. By digging out and examining old experiments, we identify the pyrochlore  $\text{Nd}_2\text{Sn}_2\text{O}_7$  as a Coulombic antiferromagnet. This novel and exotic state carries both antiferromagnetic order and emergent quantum electrodynamics with gapless gauge photon and fractionalized quasiparticles. The antiferromagnetic order and the gauge photon naturally explain the neutron diffraction result and the anomalously large  $T^3$  specific heat, respectively. We propose the representative dynamical properties for the Coulombic antiferromagnet that can be examined by the inelastic neutron scattering measurements. If the experiment in  $\text{Nd}_2\text{Sn}_2\text{O}_7$  can be repeated,  $\text{Nd}_2\text{Sn}_2\text{O}_7$  might become the first Coulombic antiferromagnet with a visible emergent gauge photon and thus an unique system with both the long-range order and the long-range entanglement. We also expect this work to inspire interests in the search of exotic physics in ordered magnets.

Exotic quantum states of matter with long-range quantum entanglement such as fractional quantum Hall effects and quantum spin liquids are characterized by emergent gauge fields and fractionalized excitations [1]. Due to the emergent non-local gauge structures, these states are usually robust against weak local perturbations. Moreover, the emergent gauge field and fractionalization could survive even in the presence of long-range orders. This happens, for example when the residual interactions between the fractionalized quasiparticles induce the condensation of composite objects without completely destroying the internal gauge structures. Such a scenario was theoretically proposed about twenty years ago for the superconducting cuprates where the hosting exotic state was suggested to be  $\mathbb{Z}_2$  topological order [2–5]. Over there, the bilinear of the fermionic spinons was condensed to generate the antiferromagnetic long-range order while the fractionalization and the  $\mathbb{Z}_2$  gauge structure persist. To distinguish it from the conventional antiferromagnet, this fractionalized antiferromagnet was dubbed “AF\* state”. Although its connection to the cuprates remains illusive, such an exotically ordered state points to the important possibility of emergent exotic physics in the seemingly ordered systems, i.e. the coexistence of long-range order with long-range entanglement.

Despite the possibility of exoticity in the long-range ordered systems, the popular search of exotic physics is to examine spin liquid candidates among disordered magnets with frustration such that the frustration enhances the quantum fluctuations and suppresses the magnetic orders down to zero temperature [6, 7]. In this Letter, we point out that the seemingly ordered pyrochlore  $\text{Nd}_2\text{Sn}_2\text{O}_7$  is likely to be a realistic and rare example of exotically ordered magnet where the emergent gauge field and the fractionalization coexist with the antiferromagnetic order. The pyrochlore magnets have been an active topic in the modern research of quantum magnetism and have attracted quite some attention in last two decades [8, 9]. The classical spin ice has been observed in the pyrochlore spin ice magnets and understood based on

the interacting Ising spins [10–13]. The quantum counterpart, referred as pyrochlore quantum spin ice or pyrochlore ice  $U(1)$  spin liquid, is less conclusive [6, 14–17]. There have been two kinds of relevant models [6, 15, 16, 18–21]. Due to the low energy scales of the emergent excitations such as the gauge photons and the fractionalized excitations, the experimental side is less conclusive compared to the classical case. So far, the existing candidates that remain disordered and promising are the Tb-based [22], Pr-based pyrochlores [23, 24] with the non-Kramers doublets, and more recently the Ce-based pyrochlores with the dipole-octupole (DO) doublets [25–33]. The challenge is to establish a close connection between theory and experiments and to identify the qualitative or smoking-gun signatures of exotic properties.

We outline the existing but unexplored phenomena of  $\text{Nd}_2\text{Sn}_2\text{O}_7$  that inspired us. The  $\text{Nd}^{3+}$  ions form a pyrochlore lattice. Like other Nd-based pyrochlores including  $\text{Nd}_2\text{Zr}_2\text{O}_7$  and  $\text{Nd}_2\text{Hf}_2\text{O}_7$  [34–38],  $\text{Nd}_2\text{Sn}_2\text{O}_7$  develops the “all-in all-out” antiferromagnetic order, and the ordering temperature  $T_N$  is  $\sim 0.91\text{K}$  [39]. Remarkably, the specific heat below  $T_N$  behaves like  $T^3$  and thus supports low-energy gapless modes [39, 40]. Due to the small energy scale of the interaction, this magnetic specific heat is several orders of magnitude higher than the phonon contribution. We think these results are difficult to reconcile with the existing theories and our understanding of the rare-earth magnets. For such a well-ordered magnet, the low-energy excitations would be simple magnons. In the rare-earth magnets, the spin model that governs the physics of the local moments usually has a very low symmetries. These symmetries are discrete and include the lattice symmetry and the time reversal due to the spin-orbit-coupled nature of most local moments. For the  $\text{Nd}^{3+}$  ion, more microscopic information was known. The ground state Kramers doublet is well separated from the excited ones by a crystal field gap of  $26\text{meV}$  [39] such that the effective spin-1/2 local moment from the ground state gives a good description of the magnetic properties below  $\sim 20\text{K}$ . Moreover, the  $\text{Nd}^{3+}$

ground state Kramers doublet is the DO doublet [19, 28]. Therefore, the effective model between these spin-1/2 moments is understood, and clearly does not have any continuous symmetry to support gapless Goldstone modes. Furthermore, the relevant model has already been shown to produce the “all-in all-out” order in some parameter regime [19], and this ordered regime does not have the quantum order by disorder effect that would support nearly gapless pseudo-Goldstone modes [41]. The latter could lead to a nearly  $T^3$  heat capacity and has been proposed for  $\text{Er}_2\text{Ti}_2\text{O}_7$  [42, 43].

To reconcile the puzzling experiments, we assert that, the ground state of  $\text{Nd}_2\text{Sn}_2\text{O}_7$  is a Coulombic antiferromagnet. This state is analogous to the  $\text{AF}^*$  state for the cuprates. Thus, we also refer this exotic state as “pyrochlore  $\text{AF}^*$  state”. It is a novel state of matter where the long-range antiferromagnetic order coexists with the three-dimensional U(1) topological order, i.e. the coexistence of long-range order and the long-range entanglement. The long-range order in  $\text{Nd}_2\text{Sn}_2\text{O}_7$  is the antiferromagnetic “all-in all-out” order, and the gapless U(1) gauge photon of the three-dimensional U(1) topological order accounts for the anomalously large  $T^3$  heat capacity. The emergence of such an exotic state raises two questions. The first question is whether the relevant model could support the pyrochlore  $\text{AF}^*$  state as one possible ground state. This is certainly difficult as the model cannot be well solved. In the unfrustrated regime where the nearest-neighbor part of the model can be well-understood, no such state was found [19, 28]. Thus, extra interactions and/or the frustrated regime are required to support its existence. The second question is about the important physical consequences of this exotic state. Besides the existing thermodynamics, what are other key properties that can be used to pin down the assertion about this exotic state in  $\text{Nd}_2\text{Sn}_2\text{O}_7$ ?

The generic spin model for the Nd-based DO doublet in  $\text{Nd}_2\text{Sn}_2\text{O}_7$  is given as follows,

$$H = \sum_{\langle ij \rangle} \left[ J_x S_i^x S_j^x + J_z S_i^z S_j^z + J_{xz} (S_i^x S_j^z + S_i^z S_j^x) + J_y S_i^y S_j^y \right] - \sum_{\langle\langle ij \rangle\rangle} J_2 S_i^z S_j^z + \dots, \quad (1)$$

where the pseudospin  $S_i$  is defined on the DO doublet and  $\langle ij \rangle$  ( $\langle\langle ij \rangle\rangle$ ) refers to the nearest (second) neighbors. The terms inside “[ ]” of Eq. (1) are the most general symmetry-allowed interactions between the nearest neighbors, while “...” refers to other interactions such as the dipole-dipole interaction between the  $S^z$ -component and the superexchange beyond nearest neighbors. As we have previously remarked, the nearest-neighbor model seems insufficient at least in the unfrustrated regime [19, 28]. We need extra interactions, and we include a second-neighbor  $S^z$ - $S^z$  interaction for illustration.

Microscopically [19], the  $S^z$  ( $S^x$  or  $S^y$ ) component for the DO doublet carries the magnetic dipole (octupole) moment. One should only keep the  $S^z$ - $S^z$  coupling if the dipole-dipole interaction is considered. From the symmetry analysis, however,  $S^z$  and  $S^x$  ( $S^y$ ) transform identically as a magnetic

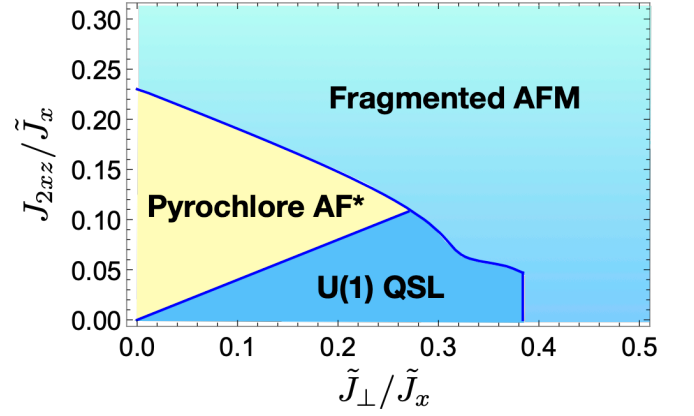


FIG. 1. (Color online.) Phase diagram for  $H_a$  in Eq. (7). The phase boundary between the pyrochlore  $\text{AF}^*$  state and the fragmented AFM is continuous via the spinon condensation. The remaining phase boundaries are all first order. U(1) QSL refers to the pyrochlore U(1) spin liquid. The  $\text{AF}^*$  state is also referred as Coulombic antiferromagnet.

dipole (octupole) under the space group. This is the symmetry reason why there exists the  $S^x$ - $S^z$  coupling in Eq. (1). If one restricts to the nearest-neighbor model, one can apply a rotation about the  $y$ -axis to eliminate the crossing term between  $S^x$  and  $S^z$ . With the further-neighbor interactions, it becomes impossible because such a rotation immediately re-generates the crossing terms from the further neighbors. After the rotation, Eq. (1) takes a new form,

$$H = \sum_{\langle ij \rangle} \left[ \tilde{J}_x \tilde{S}_i^x \tilde{S}_j^x + \tilde{J}_z \tilde{S}_i^z \tilde{S}_j^z + J_y S_i^y S_j^y \right] - \sum_{\langle\langle ij \rangle\rangle} J_2 \left[ \cos^2 \theta \tilde{S}_i^z \tilde{S}_j^z + \sin^2 \theta \tilde{S}_i^x \tilde{S}_j^x + \cos \theta \sin \theta (\tilde{S}_i^z \tilde{S}_j^z + \tilde{S}_i^x \tilde{S}_j^x) \right] + \dots, \quad (2)$$

where  $\tilde{S}_i^x = \cos \theta S_i^x + \sin \theta S_i^z$ ,  $\tilde{S}_i^z = \cos \theta S_i^z - \sin \theta S_i^x$ ,  $\tilde{J}_x$  and  $\tilde{J}_z$  are the rotated couplings and are related to the old ones [25], and the crossing term reappears. As we show below, the irremovable crossing term is responsible for the emergence of the pyrochlore  $\text{AF}^*$  state from the U(1) spin liquid. Since other interactions in “...” necessarily renormalize the  $J_2$  interactions, to capture the qualitative physics, we consider an alternative model with the renormalized couplings,

$$H_a = \sum_{\langle ij \rangle} \left[ \tilde{J}_x \tilde{S}_i^x \tilde{S}_j^x - \tilde{J}_\perp (\tilde{S}_i^z \tilde{S}_j^z + S_i^y S_j^y) \right] - \sum_{\langle\langle ij \rangle\rangle} J_{2xz} (\tilde{S}_i^x \tilde{S}_j^z + \tilde{S}_i^z \tilde{S}_j^x). \quad (3)$$

We have set  $\tilde{J}_z = J_y = -\tilde{J}_\perp$  to avoid further complication.  $H_a$  is our minimal model to reveal the pyrochlore  $\text{AF}^*$  state.

We start from the large antiferromagnetic  $\tilde{J}_x$  regime and consider the instability to the nearby phases. With the large antiferromagnetic  $\tilde{J}_x$ , the system prefers the “two-plus two-minus” ice configuration for  $\tilde{S}^x$  and realizes a pyrochlore U(1)

spin liquid with the perturbed quantum fluctuations. This is a reasonable starting point because both the pyrochlore U(1) spin liquid and the AF\* state share the same gauge structure. In this limit, the system is characterized by the emergent U(1) gauge field and the fractionalized excitations. To reveal it, we implement the spinon-gauge construction and express the spin operators as [16, 19, 20]

$$\begin{aligned}\tilde{S}_{\mathbf{r},\mathbf{r}+e_\mu}^+ &\equiv \tilde{S}_{\mathbf{r},\mathbf{r}+e_\mu}^z - iS_{\mathbf{r},\mathbf{r}+e_\mu}^y = \Phi_{\mathbf{r}}^\dagger \Phi_{\mathbf{r}+e_\mu} \tilde{s}_{\mathbf{r},\mathbf{r}+e_\mu}^+, \quad (4) \\ \tilde{S}_{\mathbf{r},\mathbf{r}+e_\mu}^x &= \tilde{s}_{\mathbf{r},\mathbf{r}+e_\mu}^x, \quad (5)\end{aligned}$$

where the pyrochlore spin is now interpreted as sitting on a link connecting the centers  $\mathbf{r}$  and  $\mathbf{r} + e_\mu$  of the neighboring tetrahedra. The tetrahedral centers form a diamond lattice, and

$e_\mu$  refers to the four nearest-neighbor vectors that connect the I sublattice sites to the II sublattice sites. Here  $\tilde{s}_{\mathbf{r},\mathbf{r}+e_\mu}$  is a spin-1/2 variable that corresponds to the emergent U(1) gauge field. The spinons carry the emergent gauge charge, and  $\Phi_{\mathbf{r}}^\dagger$  ( $\Phi_{\mathbf{r}}$ ) creates (annihilates) a spinon at the diamond site  $\mathbf{r}$  such that the spinon number  $Q_{\mathbf{r}}$  satisfies

$$[\Phi_{\mathbf{r}}, Q_{\mathbf{r}'}] = \Phi_{\mathbf{r}} \delta_{\mathbf{r}\mathbf{r}'}, \quad [\Phi_{\mathbf{r}}^\dagger, Q_{\mathbf{r}'}] = -\Phi_{\mathbf{r}}^\dagger \delta_{\mathbf{r}\mathbf{r}'}. \quad (6)$$

As the Hilbert space is enlarged by the spinon-gauge construction, the constraint  $Q_{\mathbf{r}} = \eta_{\mathbf{r}} \sum_{\mu} \tilde{s}_{\mathbf{r},\mathbf{r}+\eta_{\mathbf{r}}e_\mu}^x$  is imposed. The spinon-gauge construction captures the nature of the pyrochlore U(1) spin liquid as a string-net condensed phase [44], where  $\tilde{S}_i^\pm$  corresponds to the shortest open string with the spinons at the two ends. The model  $H_a$  becomes

$$H_a = \sum_{\mathbf{r}} \frac{\tilde{J}_x}{2} Q_{\mathbf{r}}^2 - \sum_{\mathbf{r}} \sum_{\mu \neq \nu} \frac{\tilde{J}_\perp}{2} \Phi_{\mathbf{r}+\eta_{\mathbf{r}}e_\mu}^\dagger \Phi_{\mathbf{r}+\eta_{\mathbf{r}}e_\nu} \tilde{s}_{\mathbf{r},\mathbf{r}+\eta_{\mathbf{r}}e_\mu}^{-\eta_{\mathbf{r}}} \tilde{s}_{\mathbf{r},\mathbf{r}+\eta_{\mathbf{r}}e_\nu}^{+\eta_{\mathbf{r}}} - \sum_{\mathbf{r} \in \text{I}} \sum_{\mu} \sum_{j \in [\mathbf{r},\mathbf{r}+e_\mu]_2} \frac{J_{2xz}}{2} (\Phi_{\mathbf{r}}^\dagger \Phi_{\mathbf{r}+e_\mu} \tilde{s}_{\mathbf{r},\mathbf{r}+e_\mu}^+ + h.c.) \tilde{s}_j^x \quad (7)$$

where  $[\mathbf{r}, \mathbf{r} + e_\mu]_2$  refers to the set of the second neighbors from this site at  $\mathbf{r} + e_\mu/2$ . To solve  $H_a$ , we decouple it into the spinon sector and the gauge field sector with

$$H_{\text{spinon}} = \sum_{\mathbf{r}} \frac{\tilde{J}_x}{2} Q_{\mathbf{r}}^2 - \sum_{\mathbf{r}} \sum_{\mu \neq \nu} \frac{1}{2} \tilde{J}_\perp \chi_1 \Phi_{\mathbf{r}+\eta_{\mathbf{r}}e_\mu}^\dagger \Phi_{\mathbf{r}+\eta_{\mathbf{r}}e_\nu} - \sum_{\mathbf{r} \in \text{I}} \sum_{\mu} 6J_{2xz} \chi_2 (\Phi_{\mathbf{r}}^\dagger \Phi_{\mathbf{r}+e_\mu} + \Phi_{\mathbf{r}+e_\mu}^\dagger \Phi_{\mathbf{r}}), \quad (8)$$

$$H_{\text{gauge}} = - \sum_{\langle ij \rangle} \tilde{J}_\perp I_1 (\tilde{s}_i^z \tilde{s}_j^z + s_i^y s_j^y) - \sum_{\langle\langle ij \rangle\rangle} J_{2xz} I_2 (\tilde{s}_i^x \tilde{s}_j^z + \tilde{s}_i^z \tilde{s}_j^x), \quad (9)$$

where  $\chi_1 = \langle \tilde{s}_i^+ \tilde{s}_j^- \rangle$  for  $\langle ij \rangle$  and  $\chi_2 = \langle \tilde{s}_i^+ \tilde{s}_j^x \rangle$  for  $\langle\langle ij \rangle\rangle$ , and  $I_1 = \langle \Phi_{\mathbf{r}}^\dagger \Phi_{\mathbf{r}'} \rangle$  for  $\langle\langle \mathbf{r}\mathbf{r}' \rangle\rangle$  and  $I_2 = \langle \Phi_{\mathbf{r}}^\dagger \Phi_{\mathbf{r}'} \rangle$  for  $\langle \mathbf{r}\mathbf{r}' \rangle$ . These parameters are solved self-consistently in the Supplementary material. The gauge mean-field phase diagram is depicted in Fig. 1. Two exotic phases, the U(1) spin liquid and the AF\* state, occupy the regions with small  $\tilde{J}_\perp$  and  $J_{2xz}$ . The transition between these two states in Fig. 1 is first order. Both states have gapped spinons and gapless U(1) gauge photon, while the AF\* state has an antiferromagnetic all-in all-out order. The fragmented AFM in Fig. 1 is a conventional antiferromagnet with an all-in all-out order, and can be obtained from the AF\* state via the spinon condensation at  $\Gamma$  point. Such a transition is a Higgs' transition. The visible part of the magnetic order is in the  $S^z$  component and behaves as

$$\begin{aligned}\langle S_i^z \rangle &= \cos \theta \langle \tilde{S}_i^z \rangle + \sin \theta \langle \tilde{S}_i^x \rangle \\ &= \frac{1}{2} \cos \theta [\langle \Phi_{\mathbf{r}}^\dagger \Phi_{\mathbf{r}'} \rangle \langle \tilde{s}_{\mathbf{r}\mathbf{r}'}^+ \rangle + h.c.] + \sin \theta \langle \tilde{s}_i^x \rangle. \quad (10)\end{aligned}$$

As  $S^x$  also develops order but is invisible or hidden due to the multipolar nature, the ‘‘fragmented AFM’’ is used to capture this moment fragmentation. Moreover,  $S^z$ , despite being ordered, could simultaneously function as a disordering operator to flip  $S^x$  order and generate magnetic excitations.

From Eq. (10), it is clear that the all-in all-out ( $S^z$ ) order appears when there exist the spinon tunneling between two

diamond sublattices and/or a non-vanishing emergent gauge field. Due to the generic coupling between  $S^x$  and  $S^z$  or between  $\tilde{S}^x$  and  $\tilde{S}^z$ , these two conditions are actually concomitant. In the above, we have explicitly shown that the AF\* state appears from the irremovable coupling between  $\tilde{S}^x$  and  $\tilde{S}^z$  and supports both contributions in Eq. (10) non-vanishing. It is also possible that, the spinon interaction leads to the condensation in the spinon particle-hole channel and results in an antiferromagnetic order. The key physical properties of the pyrochlore AF\* state, however, are independent from the physical origin and are discussed below.

Despite the presence of the all-in all-out order, the quantum fluctuations of the AF\* state are still governed by the frac-

Phases	$\langle \Phi \rangle$	$\langle \tilde{s}^x \rangle$	$\langle \tilde{s}^\pm \rangle$	$\langle S^x \rangle$	$\langle S^z \rangle$
U(1) QSL	= 0	= 0	$\neq 0$	= 0	= 0
AF* state	= 0	$\neq 0$	$\neq 0$	$\neq 0$	$\neq 0$
Fragmented AFM	$\neq 0$	$\neq 0$	$\neq 0$	$\neq 0$	$\neq 0$

TABLE I. Description of each phase within gauge mean-field theory in Fig. 1.

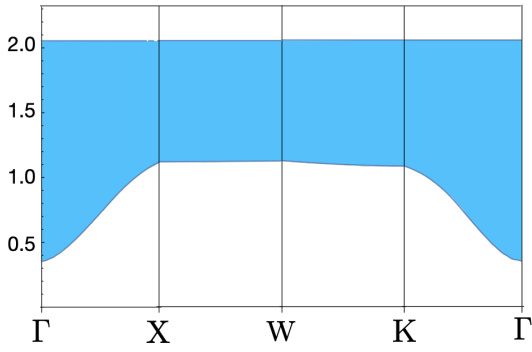


FIG. 2. Spinon continuum along the high symmetry momentum lines of the pyrochlore AF\* state. Here  $t_1 = 0.025$ ,  $t_2 = 0.02$ , and  $\tilde{J}_x$  is set to unity.

tionalized spinons and the emergent U(1) gauge fluctuations. Thus, the gapless U(1) gauge photon is responsible for the  $T^3$  specific heat. We further explore the spectroscopic consequences of the AF\* state. This can be analyzed from a more phenomenological treatment that introduces the all-in all-out order on top of the fractionalized spin liquid state. The resulting spinon Hamiltonian will be of an identical structure as Eq. (8), and we write it down here,

$$H_{AF^*} = \sum_{\mathbf{r}} \frac{\tilde{J}_x}{2} Q_{\mathbf{r}}^2 - \sum_{\mathbf{r}} \sum_{\mu \neq \nu} t_1 \Phi_{\mathbf{r}+\eta_{\mathbf{r}}\mathbf{e}_{\mu}}^{\dagger} \Phi_{\mathbf{r}+\eta_{\mathbf{r}}\mathbf{e}_{\nu}} - \sum_{\mathbf{r} \in 1} \sum_{\mu} t_2 (\Phi_{\mathbf{r}}^{\dagger} \Phi_{\mathbf{r}+\mathbf{e}_{\mu}} + \Phi_{\mathbf{r}+\mathbf{e}_{\mu}}^{\dagger} \Phi_{\mathbf{r}}), \quad (11)$$

where the inter-sublattice hopping  $t_2 \neq 0$  when the magnetic order is present. This is a bit different from the case without the sublattice mixing where the spinon number is separately conserved on each diamond sublattice and the two spinon bands are degenerate. Here the two spinon dispersions are

$$\omega_{\pm}(\mathbf{k}) = \sqrt{2\tilde{J}_x} \left[ \lambda - t_1 \sum_n \cos(\mathbf{k} \cdot \mathbf{a}_n) \pm t_2 \left| \sum_{\mu} e^{i\mathbf{k} \cdot \mathbf{e}_{\mu}} \right| \right]^{\frac{1}{2}}, \quad (12)$$

where  $\{\mathbf{a}_n\}$  refers to twelve second-neighbor vectors on the diamond lattice, and  $\lambda$  is the Lagrangian multiplier used to fix the constraint  $|\Phi_{\mathbf{r}}^2| = 1$  and determined self-consistently. The spinon-pair excitations are included in the  $\tilde{S}^x$ - $\tilde{S}^x$  correlation and can be detected in the inelastic neutron scattering measurement. From the energy-momentum conservation, the spinon-pair excitation is characterized with the energy-momentum relation,  $\Omega(\mathbf{q}) = \omega_{\mu}(\mathbf{k}_1) + \omega_{\nu}(\mathbf{q} - \mathbf{k}_1)$ , where  $\mu, \nu = \pm$  refer to the spinon branches. Due to the freedom of the spinon momentum  $\mathbf{k}_1$ , the above excitation corresponds to a continuum in both energy and momentum domains. In Fig. 2, we plot the momentum-resolved energy range of the spinon continuum.

Apart from the gapped spinon continuum and the gapless gauge photon in the dynamics, there also exists the electric monopole continuum in the  $\tilde{S}^x$ - $\tilde{S}^x$  correlation [45, 46]. Moreover, because  $\langle \tilde{S}^x \rangle \neq 0$  in the AF\* state, the background dual

U(1) gauge flux is deviated from the  $\pi$  flux, and the electric monopole will have a Hofstadter band structure that can be manifested in the monopole continuum [47]. As the physical observable is the  $\tilde{S}^z$ - $\tilde{S}^z$  correlation that contains both  $\tilde{S}^z$ - $\tilde{S}^z$  and  $\tilde{S}^x$ - $\tilde{S}^x$  correlations [28], the spectral weights of the continuum for both the spinons and the electric monopoles as well as the gauge photon can be weak. What is more, the spectral weight of the gauge photon scales linearly with the energy and is suppressed at lower energies [20, 48]. Nevertheless, these emergent parton-gauge dynamics are fundamentally different from the simple magnons for a conventionally ordered magnet. As a comparison, we further plot the magnon dispersion for the fragmented AFM in the Supplementary material. Among the four magnon branches, two are flat bands, and the other two are dispersive.

*Discussion.*—As the pyrochlore AF\* state carries an antiferromagnetic order, there should exist a finite-temperature phase transition. The antiferromagnetic order occurs in the particle-hole channel of the spinons and does not carry any emergent gauge charge. Thus, the Ginzburg-Landau theory for such a transition is absent of the gauge degrees of freedom, and we expect this transition to be a conventional Ising transition in three dimensions. The magnetic transition [40] in  $\text{Nd}_2\text{Sn}_2\text{O}_7$  was found to be continuous [39]. It would be illuminating to examine the critical exponents at the transition. Below the ordering transition,  $\text{Nd}_2\text{Sn}_2\text{O}_7$  shows an anomalously large  $T^3$  specific heat, and Ref. 39 expected a linearly dispersive mode with an excitation velocity  $v_{\text{ex}} = 55\text{m/s}$ . If our assertion of the pyrochlore AF\* state for  $\text{Nd}_2\text{Sn}_2\text{O}_7$  is right, this would be the first time measurement of the emergent gauge photon in a quantum many-body system, and  $v_{\text{ex}}$  is nothing but the speed of emergent light. Moreover, it will be the first time to manifest the realization of emergent gauge structure from the microscopic systems without any gauge degree of freedom. To further confirm our assertion, we have suggested the inelastic neutron scattering measurement to directly detect the gauge photon as well as the continuum of the spinons and the electric monopoles.

In contrast to  $\text{Nd}_2\text{Sn}_2\text{O}_7$ ,  $\text{Nd}_2\text{Zr}_2\text{O}_7$  and  $\text{Nd}_2\text{Hf}_2\text{O}_7$  are deep in the conventionally ordered regime and manifested as an “all-in all-out” order in the  $S^z$  component and the associated spin wave modes [34–38]. As the actual order also involves the hidden  $S^x$  component, the  $S^z$  operator is then responsible for flipping the order in  $S^x$  in addition to having the order within itself. This interesting moment fragmentation [49] arises from the  $J_{xz}$  crossing term [19] in Eq. (1), and has been well-understood from the peculiar microscopic properties and the model Hamiltonian for the DO doublets of the  $\text{Nd}^{3+}$  ions [34, 35, 37]. Here we do not get into too much details. Another Nd-compound  $\text{Nd}_2\text{GaSbO}_7$  with the “all-in all-out” order was experimentally studied and the moment fragmentation physics was absent [50]. The onset of a continuum-like feature below the ordering transition seems more compatible with the spinon continuum of the pyrochlore AF\* state. Due to the intrinsic disorder in the system, more information needs to be collected and examined.



*Acknowledgments.*—This work is supported by the National Science Foundation of China with Grant No. 92065203, the Ministry of Science and Technology of China with Grants No. 2021YFA1400300, by the Shanghai Municipal Science and Technology Major Project with Grant No. 2019SHZDZX01, and by the Research Grants Council of Hong Kong with General Research Fund Grant No. 17306520.

\* [gangchen@hku.hk](mailto:gangchen@hku.hk)

- [1] X.-G. Wen, *Quantum field theory of many-body systems: from the origin of sound to an origin of light and electrons* (Oxford University Press, Oxford, 2007).
- [2] T. Senthil and Matthew P. A. Fisher, “ $Z_2$  gauge theory of electron fractionalization in strongly correlated systems,” *Phys. Rev. B* **62**, 7850–7881 (2000).
- [3] Leon Balents, Matthew P. A. Fisher, and Chetan Nayak, “Dual order parameter for the nodal liquid,” *Phys. Rev. B* **60**, 1654–1667 (1999).
- [4] C. Lannert and Matthew P. A. Fisher, “Inelastic Neutron Scattering Signal from Deconfined Spinons in a Fractionalized Antiferromagnet,” *International Journal of Modern Physics B* **17**, 2821–2838 (2003), [arXiv:cond-mat/0204382 \[cond-mat.str-el\]](https://arxiv.org/abs/cond-mat/0204382).
- [5] C. Lannert, Matthew P. A. Fisher, and T. Senthil, “Electron spectral function in two-dimensional fractionalized phases,” *Phys. Rev. B* **64**, 014518 (2001).
- [6] Lucile Savary and Leon Balents, “Quantum spin liquids: a review,” *Reports on Progress in Physics* **80**, 016502 (2016).
- [7] J. Knolle and R. Moessner, “A field guide to spin liquids,” *Annual Review of Condensed Matter Physics* **10**, 451–472 (2019).
- [8] Jason S. Gardner, Michel J. P. Gingras, and John E. Greedan, “Magnetic pyrochlore oxides,” *Rev. Mod. Phys.* **82**, 53–107 (2010).
- [9] Jeffrey G. Rau and Michel J.P. Gingras, “Frustrated quantum rare-earth pyrochlores,” *Annual Review of Condensed Matter Physics* **10**, 357–386 (2019).
- [10] Steven T. Bramwell and Michel J. P. Gingras, “Spin ice state in frustrated magnetic pyrochlore materials,” *Science* **294**, 1495–1501 (2001).
- [11] C. Castelnovo, R. Moessner, and S. L. Sondhi, “Magnetic monopoles in spin ice,” *Nature* **451**, 42–45 (2008).
- [12] Michel J. P. Gingras, “Observing monopoles in a magnetic analog of ice,” *Science* **326**, 375–376 (2009).
- [13] Oleg Tchernyshyov, “Magnetism: Freedom for the poles,” *Nature* **451**, 22–23 (2008).
- [14] Michael Hermele, Matthew P. A. Fisher, and Leon Balents, “Pyrochlore photons: The  $U(1)$  spin liquid in a  $S = \frac{1}{2}$  three-dimensional frustrated magnet,” *Phys. Rev. B* **69**, 064404 (2004).
- [15] M J P Gingras and P A McClarty, “Quantum spin ice: a search for gapless quantum spin liquids in pyrochlore magnets,” *Reports on Progress in Physics* **77**, 056501 (2014).
- [16] SungBin Lee, Shigeki Onoda, and Leon Balents, “Generic quantum spin ice,” *Phys. Rev. B* **86**, 104412 (2012).
- [17] Steven T Bramwell and Mark J Harris, “The history of spin ice,” *Journal of Physics: Condensed Matter* **32**, 374010 (2020).
- [18] Kate A. Ross, Lucile Savary, Bruce D. Gaulin, and Leon Balents, “Quantum Excitations in Quantum Spin Ice,” *Phys. Rev. X* **1**, 021002 (2011).
- [19] Yi-Ping Huang, Gang Chen, and Michael Hermele, “Quantum Spin Ices and Topological Phases from Dipolar-Octupolar Doublets on the Pyrochlore Lattice,” *Phys. Rev. Lett.* **112**, 167203 (2014).
- [20] Lucile Savary and Leon Balents, “Coulombic Quantum Liquids in Spin-1/2 Pyrochlores,” *Phys. Rev. Lett.* **108**, 037202 (2012).
- [21] Shigeki Onoda and Yoichi Tanaka, “Quantum fluctuations in the effective pseudospin- $\frac{1}{2}$  model for magnetic pyrochlore oxides,” *Phys. Rev. B* **83**, 094411 (2011).
- [22] Hamid R. Molavian, Michel J. P. Gingras, and Benjamin Canals, “Dynamically Induced Frustration as a Route to a Quantum Spin Ice State in  $Tb_2Ti_2O_7$  via Virtual Crystal Field Excitations and Quantum Many-Body Effects,” *Phys. Rev. Lett.* **98**, 157204 (2007).
- [23] K Kimura, S Nakatsuji, J-J Wen, C Broholm, M B Stone, E Nishibori, and H Sawa, “Quantum fluctuations in spin-ice-like  $Pr_2Zr_2O_7$ ,” *Nat. Commun.* **4**, 1934 (2013).
- [24] R Sibille, N Gauthier, H Yan, M Ciomaga Hatnean, J Ollivier, B Winn, U Filges, G Balakrishnan, M Kenzelmann, N Shannon, and T Fennell, “Experimental signatures of emergent quantum electrodynamics in  $Pr_2Hf_2O_7$ ,” *Nat. Phys.* **14**, 711 (2018).
- [25] Romain Sibille, Elsa Lhotel, Vladimir Pomjakushin, Chris Baines, Tom Fennell, and Michel Kenzelmann, “Candidate Quantum Spin Liquid in the  $Ce^{3+}$  Pyrochlore Stannate  $Ce_2Sn_2O_7$ ,” *Phys. Rev. Lett.* **115**, 097202 (2015).
- [26] J. Gaudet, E. M. Smith, J. Dudemaine, J. Beare, C. R. C. Buhariwalla, N. P. Butch, M. B. Stone, A. I. Kolesnikov, Guangyong Xu, D. R. Yahne, K. A. Ross, C. A. Marjerrison, J. D. Garrett, G. M. Luke, A. D. Bianchi, and B. D. Gaulin, “Quantum Spin Ice Dynamics in the Dipole-Octupole Pyrochlore Magnet  $Ce_2Zr_2O_7$ ,” *Phys. Rev. Lett.* **122**, 187201 (2019).
- [27] Bin Gao, Tong Chen, David W. Tam, Chien-Lung Huang, Kalyan Sasmal, Devashibhai T. Adroja, Feng Ye, Huibo Cao, Gabriele Sala, Matthew B. Stone, Christopher Baines, Joel A. T. Verezhak, Haoyu Hu, Jae-Ho Chung, Xianghan Xu, Sang-Wook Cheong, Manivannan Nallaiyan, Stefano Spagna, M. Brian Maple, Andriy H. Nevidomskyy, Emilia Morosan, Gang Chen, and Pengcheng Dai, “Experimental signatures of a three-dimensional quantum spin liquid in effective spin-1/2  $Ce_2Zr_2O_7$  pyrochlore,” *Nature Physics* **15**, 1052–1057 (2019).
- [28] Yao-Dong Li and Gang Chen, “Symmetry enriched  $U(1)$  topological orders for dipole-octupole doublets on a pyrochlore lattice,” *Phys. Rev. B* **95**, 041106 (2017).
- [29] Xu-Ping Yao, Yao-Dong Li, and Gang Chen, “Pyrochlore  $U(1)$  spin liquid of mixed-symmetry enrichments in magnetic fields,” *Phys. Rev. Research* **2**, 013334 (2020).
- [30] Romain Sibille, Nicolas Gauthier, Elsa Lhotel, Victor Porée, Vladimir Pomjakushin, Russell A. Ewings, Toby G. Perring, Jacques Ollivier, Andrew Wildes, Clemens Ritter, Thomas C. Hansen, David A. Keen, Gøran J. Nilsen, Lukas Keller, Sylvain Petit, and Tom Fennell, “A quantum liquid of magnetic octupoles on the pyrochlore lattice,” *Nature Physics* **16**, 546–552 (2020).
- [31] E. M. Smith, O. Benton, D. R. Yahne, B. Placke, R. Schäfer, J. Gaudet, J. Dudemaine, A. Fitterman, J. Beare, A. R. Wildes, S. Bhattacharya, T. DeLazzer, C. R. C. Buhariwalla, N. P. Butch, R. Movshovich, J. D. Garrett, C. A. Marjerrison, J. P. Clancy, E. Kermarrec, G. M. Luke, A. D. Bianchi, K. A. Ross, and B. D. Gaulin, “Case for a  $U(1)_\pi$  Quantum Spin Liquid Ground State in the Dipole-Octupole Pyrochlore  $Ce_2Zr_2O_7$ ,” *Phys. Rev. X* **12**, 021015 (2022).
- [32] Anish Bhardwaj, Shu Zhang, Han Yan, Roderich Moessner, Andriy H. Nevidomskyy, and Hitesh J. Changlani, “Sleuthing out exotic quantum spin liquidity in the pyrochlore magnet

- Ce<sub>2</sub>Zr<sub>2</sub>O<sub>7</sub>,” *npj Quantum Materials* **7** (2022), 10.1038/s41535-022-00458-2.
- [33] Adarsh S. Patri, Masashi Hosoi, and Yong Baek Kim, “Distinguishing dipolar and octupolar quantum spin ices using contrasting magnetostriction signatures,” *Phys. Rev. Research* **2**, 023253 (2020).
- [34] J. Xu, Owen Benton, A. T. M. N. Islam, T. Guidi, G. Ehlers, and B. Lake, “Order out of a Coulomb Phase and Higgs Transition: Frustrated Transverse Interactions of Nd<sub>2</sub>Zr<sub>2</sub>O<sub>7</sub>,” *Phys. Rev. Lett.* **124**, 097203 (2020).
- [35] Owen Benton, “Quantum origins of moment fragmentation in Nd<sub>2</sub>Zr<sub>2</sub>O<sub>7</sub>,” *Phys. Rev. B* **94**, 104430 (2016).
- [36] J. Xu, V. K. Anand, A. K. Bera, M. Frontzek, D. L. Abernathy, N. Casati, K. Siemensmeyer, and B. Lake, “Magnetic structure and crystal-field states of the pyrochlore antiferromagnet Nd<sub>2</sub>Zr<sub>2</sub>O<sub>7</sub>,” *Phys. Rev. B* **92**, 224430 (2015).
- [37] S. Petit, E. Lhotel, B. Canals, M. Ciomaga Hatnean, J. Ollivier, H. Mutka, E. Ressouche, A. R. Wildes, M. R. Lees, and G. Balakrishnan, “Observation of magnetic fragmentation in spin ice,” *Nature Physics* **12**, 746–750 (2016).
- [38] V. K. Anand, A. K. Bera, J. Xu, T. Herrmannsdörfer, C. Ritter, and B. Lake, “Observation of long-range magnetic ordering in pyrochlore Nd<sub>2</sub>Hf<sub>2</sub>O<sub>7</sub>: A neutron diffraction study,” *Phys. Rev. B* **92**, 184418 (2015).
- [39] A. Bertin, P. Dalmas de Réotier, B. Fåk, C. Marin, A. Yaouanc, A. Forget, D. Sheptyakov, B. Frick, C. Ritter, A. Amato, C. Baines, and P. J. C. King, “Nd<sub>2</sub>Sn<sub>2</sub>O<sub>7</sub>: An all-in–all-out pyrochlore magnet with no divergence-free field and anomalously slow paramagnetic spin dynamics,” *Phys. Rev. B* **92**, 144423 (2015).
- [40] H.W.J. Blote, R.F. Wielinga, and W.J. Huiskamp, “Heat-capacity measurements on rare-earth double oxides R<sub>2</sub>M<sub>2</sub>O<sub>7</sub>,” *Physica* **43**, 549–568 (1969).
- [41] Gang Chen and Xiaoqun Wang, “Electron quasi-itinerancy intertwined with quantum order by disorder in pyrochlore iridate magnetism,” *Phys. Rev. Research* **2**, 043273 (2020).
- [42] Lucile Savary, Kate A. Ross, Bruce D. Gaulin, Jacob P. C. Ruff, and Leon Balents, “Order by Quantum Disorder in Er<sub>2</sub>Ti<sub>2</sub>O<sub>7</sub>,” *Phys. Rev. Lett.* **109**, 167201 (2012).
- [43] M. E. Zhitomirsky, M. V. Gvozdikova, P. C. W. Holdsworth, and R. Moessner, “Quantum Order by Disorder and Accidental Soft Mode in Er<sub>2</sub>Ti<sub>2</sub>O<sub>7</sub>,” *Phys. Rev. Lett.* **109**, 077204 (2012).
- [44] Michael A. Levin and Xiao-Gang Wen, “String-net condensation: A physical mechanism for topological phases,” *Phys. Rev. B* **71**, 045110 (2005).
- [45] Gang Chen, “Dirac’s “magnetic monopoles” in pyrochlore ice U(1) spin liquids: Spectrum and classification,” *Phys. Rev. B* **96**, 195127 (2017).
- [46] Gang Chen, ““Magnetic monopole” condensation of the pyrochlore ice U(1) quantum spin liquid: Application to Pr<sub>2</sub>Ir<sub>2</sub>O<sub>7</sub> and Yb<sub>2</sub>Ti<sub>2</sub>O<sub>7</sub>,” *Phys. Rev. B* **94**, 205107 (2016).
- [47] Xiao-Tian Zhang, Yong Hao Gao, Chunxiao Liu, and Gang Chen, “Topological thermal Hall effect of magnetic monopoles in the pyrochlore U(1) spin liquid,” *Phys. Rev. Research* **2**, 013066 (2020).
- [48] Owen Benton, Olga Sikora, and Nic Shannon, “Seeing the light: Experimental signatures of emergent electromagnetism in a quantum spin ice,” *Phys. Rev. B* **86**, 075154 (2012).
- [49] M. E. Brooks-Bartlett, S. T. Banks, L. D. C. Jaubert, A. Harman-Clarke, and P. C. W. Holdsworth, “Magnetic-Moment Fragmentation and Monopole Crystallization,” *Phys. Rev. X* **4**, 011007 (2014).
- [50] S. J. Gomez, P. M. Sarte, M. Zelensky, A. M. Hallas, B. A. Gonzalez, K. H. Hong, E. J. Pace, S. Calder, M. B. Stone, Y. Su, E. Feng, M. D. Le, C. Stock, J. P. Attfield, S. D. Wilson, C. R. Wiebe, and A. A. Aczel, “Absence of moment fragmentation in the mixed B-site pyrochlore Nd<sub>2</sub>GaSbO<sub>7</sub>,” *Phys. Rev. B* **103**, 214419 (2021).
- [51] Gang Chen, “Spectral periodicity of the spinon continuum in quantum spin ice,” *Phys. Rev. B* **96**, 085136 (2017).
- [52] Owen Benton, L. D. C. Jaubert, Rajiv R. P. Singh, Jaan Oitmaa, and Nic Shannon, “Quantum Spin Ice with Frustrated Transverse Exchange: From a  $\pi$ -Flux Phase to a Nematic Quantum Spin Liquid,” *Phys. Rev. Lett.* **121**, 067201 (2018).

### 1. Conventions for the coordinates

Here we list the conventions for the coordinates for the main text and this Supplementary material. The pyrochlore lattice has four sublattices, and the coordinates of the reference points from each sublattice are given as

$$\text{0th sublattice : } \mathbf{b}_0 = (0, 0, 0), \quad (13)$$

$$\text{1st sublattice : } \mathbf{b}_1 = (0, \frac{1}{4}, \frac{1}{4}), \quad (14)$$

$$\text{2nd sublattice : } \mathbf{b}_2 = (\frac{1}{4}, 0, \frac{1}{4}), \quad (15)$$

$$\text{3rd sublattice : } \mathbf{b}_3 = (\frac{1}{4}, \frac{1}{4}, 0). \quad (16)$$

For each site on the pyrochlore lattice, there are twelve second-neighbor sites, and the connecting vectors are different for different sublattices. This information is used in the calculation of the gauge sector of the mean-field theory and the Weiss mean-field theory in Sec. 2.

The centers of the tetrahedra on the pyrochlore lattice form a diamond lattice. This is where the spinon resides. The reference points for the two diamond sublattices are

$$\text{I sublattice : } (+\frac{1}{8}, +\frac{1}{8}, +\frac{1}{8}), \quad (17)$$

$$\text{II sublattice : } (-\frac{1}{8}, -\frac{1}{8}, -\frac{1}{8}). \quad (18)$$

The four nearest-neighbor vectors on the diamond lattice are given as

$$\mathbf{e}_0 = (+\frac{1}{4}, +\frac{1}{4}, +\frac{1}{4}), \quad (19)$$

$$\mathbf{e}_1 = (+\frac{1}{4}, -\frac{1}{4}, -\frac{1}{4}), \quad (20)$$

$$\mathbf{e}_2 = (-\frac{1}{4}, +\frac{1}{4}, -\frac{1}{4}), \quad (21)$$

$$\mathbf{e}_3 = (-\frac{1}{4}, -\frac{1}{4}, +\frac{1}{4}), \quad (22)$$

where the subindices correspond to the sublattices of the pyrochlore lattice whose positions are the mid-points of the vectors.

### 2. Weiss mean-field theory

The main text is using the exotic spinon-gauge construction and treatment because we are dealing with exotic quantum phases of matter. In the phase diagram that we found there exist the conventional ordered phase like the fragmented antiferromagnet. The conventional ordered phases can be understood from the more conventional means. Thus, we here adopt the conventional Weiss type of mean-field approach to explore the ordered phases. Although the Weiss mean-field theory fails to capture the properties of the exotic states, it is helpful to ensure the ground for the fully ordered phases in

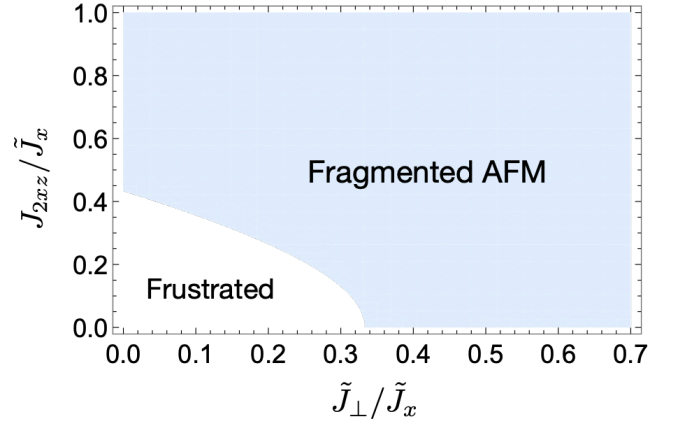


FIG. 3. Phase diagram from the Weiss mean-field theory. “Frustrated” refers to the frustrated regime where the Weiss mean-field theory fails to give reliable ground states. “Fragmented AFM” is identical the “Fragmented AFM” in Fig. 1.

the phase diagram. For this purpose, we replace the spin operator as the mean-field order and consider the spin as a classical vector. The classical mean-field ground state is obtained by optimizing the energy of the Hamiltonian in the classical limit,

$$H = \sum_{\mathbf{k}} \sum_{\mu\nu} \sum_{\alpha\beta} S_{\mathbf{k},\mu}^{\alpha} M_{\mu\nu,\alpha\beta}(\mathbf{k}) S_{-\mathbf{k},\nu}^{\beta}, \quad (23)$$

where  $M(\mathbf{k})$  is the  $12 \times 12$  “exchange matrix” in the momentum space, and  $S_{\mathbf{k}}^{\mu}$  is the Fourier component of the spin vector with

$$S_i^{\alpha} = \frac{1}{\sqrt{N}} \sum_{\mathbf{k}} S_{\mathbf{k},\mu}^{\alpha} e^{i\mathbf{k} \cdot \mathbf{R}_i}. \quad (24)$$

Here  $\mathbf{R}_i$  is the coordinate of the site  $i$ ,  $i$  belongs to the  $\mu$ -th sublattice,  $N$  is the total number of unit cell. The exchange matrix is given as

$$M(\mathbf{k}) = \begin{bmatrix} T_{00}(\mathbf{k}) & T_{01}(\mathbf{k}) & T_{02}(\mathbf{k}) & T_{03}(\mathbf{k}) \\ T_{10}(\mathbf{k}) & T_{11}(\mathbf{k}) & T_{12}(\mathbf{k}) & T_{13}(\mathbf{k}) \\ T_{20}(\mathbf{k}) & T_{21}(\mathbf{k}) & T_{22}(\mathbf{k}) & T_{23}(\mathbf{k}) \\ T_{30}(\mathbf{k}) & T_{31}(\mathbf{k}) & T_{32}(\mathbf{k}) & T_{33}(\mathbf{k}) \end{bmatrix}, \quad (25)$$

where  $T_{\mu\nu}(\mathbf{k})$  is the  $3 \times 3$  exchange matrix between the  $\mu$ -th and the  $\nu$ -th sublattices. As there does not exist the coupling from the same sublattice, the diagonal matrices are all 0 with

$$T_{\mu\mu}(\mathbf{k}) = 0. \quad (26)$$

For the off-diagonal ones with  $\mu \neq \nu$ , the contribution from the nearest-neighbor interaction is simply given as

$$\cos[\mathbf{k} \cdot \mathbf{b}_{\mu} - \mathbf{k} \cdot \mathbf{b}_{\nu}] \begin{bmatrix} \tilde{J}_x & 0 & 0 \\ 0 & J_y & 0 \\ 0 & 0 & \tilde{J}_z \end{bmatrix}. \quad (27)$$

The contribution from the second neighbor interaction is more complex. There exist 12 second neighbors for each site and

they belong to different sublattices. After a careful listing, one obtains for the interaction  $\sum_{\langle\langle ij \rangle\rangle} -J_{2xz}(\tilde{S}_i^x \tilde{S}_j^z + \tilde{S}_i^z \tilde{S}_j^x)$  that, the contribution to  $T_{01}(\mathbf{k})$  is

$$2 \cos \frac{k_x}{2} \cos \left( \frac{k_y - k_z}{4} \right) \begin{bmatrix} 0 & 0 & -J_{2xz} \\ 0 & 0 & 0 \\ -J_{2xz} & 0 & 0 \end{bmatrix}, \quad (28)$$

the contribution to  $T_{02}(\mathbf{k})$  is

$$2 \cos \frac{k_y}{2} \cos \left( \frac{k_x - k_z}{4} \right) \begin{bmatrix} 0 & 0 & -J_{2xz} \\ 0 & 0 & 0 \\ -J_{2xz} & 0 & 0 \end{bmatrix}, \quad (29)$$

the contribution to  $T_{03}(\mathbf{k})$  is

$$2 \cos \frac{k_z}{2} \cos \left( \frac{k_x - k_y}{4} \right) \begin{bmatrix} 0 & 0 & -J_{2xz} \\ 0 & 0 & 0 \\ -J_{2xz} & 0 & 0 \end{bmatrix}, \quad (30)$$

the contribution to  $T_{12}(\mathbf{k})$  is

$$2 \cos \frac{k_z}{2} \cos \left( \frac{k_x + k_y}{4} \right) \begin{bmatrix} 0 & 0 & -J_{2xz} \\ 0 & 0 & 0 \\ -J_{2xz} & 0 & 0 \end{bmatrix}, \quad (31)$$

the contribution to  $T_{13}(\mathbf{k})$  is

$$2 \cos \frac{k_y}{2} \cos \left( \frac{k_x + k_z}{4} \right) \begin{bmatrix} 0 & 0 & -J_{2xz} \\ 0 & 0 & 0 \\ -J_{2xz} & 0 & 0 \end{bmatrix}, \quad (32)$$

and the contribution to  $T_{23}(\mathbf{k})$  is

$$2 \cos \frac{k_x}{2} \cos \left( \frac{k_y + k_z}{4} \right) \begin{bmatrix} 0 & 0 & -J_{2xz} \\ 0 & 0 & 0 \\ -J_{2xz} & 0 & 0 \end{bmatrix}. \quad (33)$$

By setting  $\tilde{J}_z = J_y = -\tilde{J}_\perp$ , we solve for the ground state of  $H_a$  in Eq. (3) with the Weiss mean-field theory. The phase diagram is depicted in Fig. 3. The Weiss mean-field theory should capture the physics of the ordered phase. As it is expected, with large  $\tilde{J}_\perp$  and  $J_{2xz}$ , the ground state is the fragmented AFM. This qualitative result is actually consistent with the result from the gauge mean-field theory in Fig. 1.

In the fragmented AFM, both  $\tilde{S}^x$  and  $\tilde{S}^z$  components develop uniform magnetic orders. The visible part of the order is the  $S^z$  component that is a linear combination of  $\tilde{S}^x$  and  $\tilde{S}^z$ . As the  $z$  axis is defined locally on each sublattice, although the  $\langle S^z \rangle$  is uniform, the overall state is an antiferromagnetic state. Moreover, as some portion of the ordered moment remains in the hidden octupolar part [19, 37, 49], this antiferromagnetic ordered state is referred as the ‘‘fragmented AFM’’.

In this fragmented AFM, the reason for the presence of non-vanishing  $\tilde{S}^x$  and  $\tilde{S}^z$  order is due to the crossing coupling  $J_{2xz}$ . The  $\tilde{S}^z$  order, works as an effective and uniform Zeeman coupling to the  $\tilde{S}^x$  moment through the crossing coupling

$J_{2xz}$ . Once  $\tilde{S}^z$  develops an uniform order (for example from the  $J_\perp$  coupling), it immediately polarizes  $\tilde{S}^x$  and generates a  $\tilde{S}^x$  order even when there exists a nearest-neighbor antiferromagnetic  $\tilde{S}^x$ - $\tilde{S}^x$  interaction.

### 3. Calculation for gauge mean-field theory

We sketch the calculation of the phase diagram and the spinon excitation within the gauge mean-field theory. We first consider the gauge field sector because it is much simpler than the spinon sector. The gauge field mean-field Hamiltonian is given as

$$H_{\text{gauge}} = - \sum_{\langle ij \rangle} \tilde{J}_\perp I_1 (\tilde{s}_i^z \tilde{s}_j^z + s_i^y s_j^y) - \sum_{\langle\langle ij \rangle\rangle} J_{2xz} I_2 (\tilde{s}_i^x \tilde{s}_j^z + \tilde{s}_i^z \tilde{s}_j^x). \quad (34)$$

It is clear from the spinon mean-field Hamiltonian  $H_{\text{spinon}}$ , both  $I_1$  and  $I_2$  are positive. Thus, this ferromagnetic like interaction in Eq. (34) is quite straightforward to solve with a simple classical treatment. We choose a mean-field ansatz with

$$\langle s_i^z \rangle = \frac{1}{2} \cos \phi, \quad (35)$$

$$\langle s_i^x \rangle = \frac{1}{2} \sin \phi, \quad (36)$$

where  $\phi$  should be determined. The energy of  $H_{\text{gauge}}$  is optimized by  $\phi$  that satisfies

$$\tan(2\phi) = \frac{4I_2 J_{2xz}}{I_1 \tilde{J}_\perp}. \quad (37)$$

The gauge mean-field parameters,  $\chi_1$  and  $\chi_2$ , are then obtained as

$$\chi_1 = \langle \tilde{s}_i^+ \tilde{s}_j^- \rangle = \langle \tilde{s}_i^+ \rangle \langle \tilde{s}_j^- \rangle = \frac{1}{4} \cos^2 \phi, \quad (38)$$

$$\chi_2 = \langle \tilde{s}_i^+ \tilde{s}_j^x \rangle = \langle \tilde{s}_i^+ \rangle \langle \tilde{s}_j^x \rangle = \frac{1}{4} \cos \phi \sin \phi. \quad (39)$$

Due to the ferromagnetic interaction in  $H_{\text{gauge}}$ , the mean-field parameters,  $\chi_1$  and  $\chi_2$ , are uniform throughout the lattice.

Equipped with the above results, one can proceed to solve for the spinon sector. The spinon sector Hamiltonian is given as

$$H_{\text{spinon}} = \sum_{\mathbf{r}} \frac{\tilde{J}_x}{2} Q_{\mathbf{r}}^2 - \sum_{\mathbf{r}} \sum_{\mu \neq \nu} \frac{1}{2} \tilde{J}_\perp \chi_1 \Phi_{\mathbf{r}+\eta_{\mathbf{r}} e_\mu}^\dagger \Phi_{\mathbf{r}+\eta_{\mathbf{r}} e_\nu} - \sum_{\mathbf{r} \in 1} \sum_{\mu} 6J_{2xz} \chi_2 (\Phi_{\mathbf{r}}^\dagger \Phi_{\mathbf{r}+e_\mu} + \Phi_{\mathbf{r}+e_\mu}^\dagger \Phi_{\mathbf{r}}). \quad (40)$$

It was found to be more convenient to use a rotor representation for the spinon operator such that  $\Phi_{\mathbf{r}} = e^{-i\varphi_{\mathbf{r}}}$  and  $|\Phi_{\mathbf{r}}| = 1$ . This approximation neglects the amplitude fluctuation of the spinon fields and should be reasonable in the regimes where the spinon matter drives the physics.



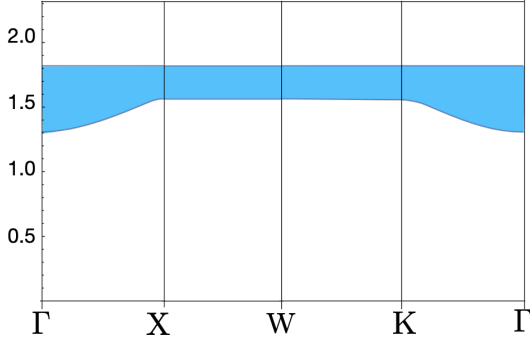


FIG. 4. Spinon continuum along the high symmetry momentum lines of the pyrochlore U(1) spin liquid. Here  $t_1 = 0.025, t_2 = 0$ , and  $\tilde{J}_x$  is set to unity. The spinon dispersion is obtained for the spinon Hamiltonian in Eq. (11).

To implement the constraint, we introduce a Lagrangian multiplier  $\lambda$  such that

$$H_{\text{spinon}} \rightarrow H_{\text{spinon}} + \sum_{\mathbf{r}} \lambda_{\mathbf{r}} (\Phi_{\mathbf{r}}^\dagger \Phi_{\mathbf{r}} - 1), \quad (41)$$

where  $\lambda_{\mathbf{r}}$  should be determined self-consistently from the modified spinon Hamiltonian and satisfy

$$\langle \Phi_{\mathbf{r}}^\dagger \Phi_{\mathbf{r}} \rangle = 1 \quad (42)$$

on every site. It is now more convenient to use path integral formulation to solve the spinon sector. In a coherent state path integral, we integrate out the ‘‘momentum-like’’ field  $Q_{\mathbf{r}}$  and establish the partition function as

$$\mathcal{Z} = \int \mathcal{D}\Phi^\dagger \mathcal{D}\Phi \mathcal{D}\lambda e^{-S} e^{-\sum_{\mathbf{r}} \int d\tau \lambda_{\mathbf{r}} (\Phi_{\mathbf{r}}^\dagger \Phi_{\mathbf{r}} - 1)}. \quad (43)$$

Here the effective action  $S$  has the form as

$$\begin{aligned} S = & \int_{d\tau} \sum_{\mathbf{r}} \frac{|\partial_\tau \Phi_{\mathbf{r}}|^2}{2\tilde{J}_x} - \sum_{\mathbf{r}} \sum_{\mu \neq \nu} \frac{1}{2} \tilde{J}_\perp \chi_1 \Phi_{\mathbf{r}+\eta_{\mathbf{r}}\mathbf{e}_\mu}^\dagger \Phi_{\mathbf{r}+\eta_{\mathbf{r}}\mathbf{e}_\nu} \\ & - \sum_{\mathbf{r} \in \Gamma} \sum_{\mu} 6J_{2xz} \chi_2 (\Phi_{\mathbf{r}}^\dagger \Phi_{\mathbf{r}+\mathbf{e}_\mu} + \Phi_{\mathbf{r}+\mathbf{e}_\mu}^\dagger \Phi_{\mathbf{r}}). \end{aligned} \quad (44)$$

In a saddle point approximation, we have  $\lambda_{\mathbf{r}} = \lambda$ . This is also demanded by the uniform state requirement.

The spinon dispersion can be immediately read off from Eq. (44) and Eq. (43), and are given as

$$\begin{aligned} \omega_{\pm}(\mathbf{k}) = & \sqrt{2\tilde{J}_x} \left[ \lambda - \frac{\tilde{J}_\perp \chi_1}{2} \sum_{\{\mathbf{a}_n\}} \cos(\mathbf{k} \cdot \mathbf{a}_n) \right. \\ & \left. \pm 6J_{2xz} \chi_2 \left| \sum_{\{\mathbf{e}_\mu\}} e^{i\mathbf{k} \cdot \mathbf{e}_\mu} \right| \right]^{1/2}, \end{aligned} \quad (45)$$

where  $\{\mathbf{e}_\mu\}$  ( $\{\mathbf{a}_n\}$ ) refers to the set of 4 first-neighbor (12 second-neighbor) vectors on the diamond lattice. In both the pyrochlore U(1) spin liquid and the pyrochlore AF\* state, the spinons are fully gapped. Once it becomes gapless, the spinons will be condensed and generate magnetism of some sorts.

The mean-field parameters,  $I_1$  and  $I_2$ , as well as the spinon amplitude, are the spinon bilinears. It is quite convenient to evaluate from the path integral approach. We find that,

$$\langle \Phi_{\mathbf{r}}^\dagger \Phi_{\mathbf{r}} \rangle = \frac{1}{2N_{u.c.}} \sum_{\mathbf{k}} \tilde{J}_x \left[ \frac{1}{\omega_+(\mathbf{k})} + \frac{1}{\omega_-(\mathbf{k})} \right], \quad (46)$$

and this quantity should be equal to 1. Here  $N_{u.c.}$  refers to the total number of unit cell. Moreover, for the second-neighbor sites  $\langle \langle \mathbf{r}\mathbf{r}' \rangle \rangle$ , we have

$$\begin{aligned} I_1 = & \langle \Phi_{\mathbf{r}}^\dagger \Phi_{\mathbf{r}'} \rangle \\ = & \frac{1}{2N_{u.c.}} \sum_{\mathbf{k}} e^{i\mathbf{k} \cdot \mathbf{a}_n} \tilde{J}_x \left[ \frac{1}{\omega_+(\mathbf{k})} + \frac{1}{\omega_-(\mathbf{k})} \right], \end{aligned} \quad (47)$$

where  $\mathbf{a}_n$  is the vector connecting  $\mathbf{r}'$  and  $\mathbf{r}$ . Due to the spatial uniformity,  $I_1$  is uniform and real. For the first-neighbor sites  $\langle \langle \mathbf{r}\mathbf{r}' \rangle \rangle$ , we have

$$\begin{aligned} I_2 = & \langle \Phi_{\mathbf{r}}^\dagger \Phi_{\mathbf{r}'} \rangle \\ = & \frac{1}{2N_{u.c.}} \sum_{\mathbf{k}} e^{-i\mathbf{k} \cdot \mathbf{e}_\nu} \frac{\sum_{\mu} e^{i\mathbf{k} \cdot \mathbf{e}_\mu}}{|\sum_{\mu} e^{i\mathbf{k} \cdot \mathbf{e}_\mu}|} \tilde{J}_x \left[ \frac{1}{\omega_-(\mathbf{k})} - \frac{1}{\omega_+(\mathbf{k})} \right], \end{aligned} \quad (48)$$

where  $\mathbf{e}_\nu$  is the vector connecting  $\mathbf{r}'$  and  $\mathbf{r}$ . Here  $I_2$  describes the inter-sublattice hopping/hybridization on the diamond lattice. It is zero in the absence of the magnetic order, and the two spinon bands are degenerate. We should emphasize that, in the calculation of  $I_1$ ,  $I_2$  and  $\langle \Phi_{\mathbf{r}}^\dagger \Phi_{\mathbf{r}} \rangle$ , we are working with the gapped spinons.

The parameters  $I_1$  and  $I_2$  are then feed back to the gauge field sector. We solve the spinon sector and the gauge field sector together self-consistently. The self-consistent mean-field results are finally determined based on their variational energy  $\langle H_a \rangle$  where  $H_a$  is given in Eq. (7). We evaluate  $\langle H_a \rangle$  with respect to the gauge mean-field states as

$$\begin{aligned} \langle H_a \rangle = & \sum_{\mathbf{r}} \langle \frac{\tilde{J}_x}{2} Q_{\mathbf{r}}^2 \rangle \\ & - \sum_{\mathbf{r}} \sum_{\mu \neq \nu} \frac{\tilde{J}_\perp}{2} \langle \Phi_{\mathbf{r}+\eta_{\mathbf{r}}\mathbf{e}_\mu}^\dagger \Phi_{\mathbf{r}+\eta_{\mathbf{r}}\mathbf{e}_\nu} \tilde{s}_{\mathbf{r},\mathbf{r}+\eta_{\mathbf{r}}\mathbf{e}_\mu}^{-\eta_{\mathbf{r}}} \tilde{s}_{\mathbf{r},\mathbf{r}+\eta_{\mathbf{r}}\mathbf{e}_\nu}^{+\eta_{\mathbf{r}}} \rangle \\ & - \sum_{\mathbf{r} \in \Gamma} \sum_{\mu} \sum_{j \in [\mathbf{r}, \mathbf{r}+\mathbf{e}_\mu]_2} \frac{J_{2xz}}{2} \langle (\Phi_{\mathbf{r}}^\dagger \Phi_{\mathbf{r}+\mathbf{e}_\mu} \tilde{s}_{\mathbf{r},\mathbf{r}+\mathbf{e}_\mu}^+ + h.c.) \tilde{s}_j^x \rangle \\ = & \sum_{\mathbf{k}} \frac{1}{2} [\omega_+(\mathbf{k}) + \omega_-(\mathbf{k})] \\ & - 12\tilde{J}_\perp \chi_1 I_1 N_{u.c.} - 48J_{2xz} I_2 \chi_2 N_{u.c.}, \end{aligned} \quad (49)$$

where in the evaluation of the first kinetic energy term, we have made use of the factor that, for each harmonic oscillator, the kinetic energy of the ground state is simply 1/2 of the total zero-point energy. As this is a complex field, we have an extra factor of 2 for the kinetic energy part. The remaining contributions are simply evaluated against their mean-field values in the real space.

#### 4. Spinons in U(1) spin liquid

The spinons in both pyrochlore U(1) spin liquid and the pyrochlore AF\* state are fully gapped. The difference is that, for the pyrochlore U(1) spin liquid under consideration in Fig. 1, the spinons are degenerate, while for the pyrochlore AF\* state, the spinons are not degenerate due to the inter-sublattice hopping from the magnetic order. As a comparison, we plot the spinon continuum for the pyrochlore U(1) spin liquid in Fig. 4. The spinon dispersion is obtained from Eq. (11) by setting  $t_2 = 0$ . This spinon dispersion is equivalent to  $\tilde{J}_\perp = 0.1\tilde{J}_x$  in Fig. 1. Although this is not a parallel comparison, the bandwidth of the spinon continuum is much reduced in the pyrochlore U(1) spin liquid.

#### 5. With dominant $\tilde{S}^z$ interaction

Throughout this paper, we have considered a predominant and frustrated  $\tilde{S}^x$  interaction and analyzed the resulting magnetic orders and phases. In fact, due to the identical symmetry property, it would be qualitatively equivalent to consider the case with a predominant and frustrated  $\tilde{S}^z$  interaction. One can still obtain the pyrochlore U(1) spin liquid, the pyrochlore AF\* and the fragmented AFM states. The procedures are identical to the ones that have been used in this paper, and the phases have qualitatively the same physical properties. The reason to select the predominant  $\tilde{S}^x$  interaction is based on the Curie-Weiss temperature. For the nearest-neighbor XYZ model for the DO doublet, we have [28]

$$\Theta_{\text{CW}} = \frac{1}{2}J_z. \quad (50)$$

The Curie-Weiss temperature of Nd<sub>2</sub>Sn<sub>2</sub>O<sub>7</sub> between 5K and 15K is  $-0.32\text{K}$  [39]. Even though the further neighbor interactions would modify Eq. (50), this still give a rough estimate that  $J_z$  is more likely to be ferromagnetic. Thus, we consider a predominant and frustrated  $\tilde{S}^x$  interaction in this paper. In the end,  $\tilde{S}^x$  and  $\tilde{S}^z$  are simply notations for calculation, only the physical  $S^x$  and  $S^z$  are meaningful.

#### 6. Spinon interactions

In this paper, we have considered the mechanism of mutual induction between the gauge link and the gauge field as the mechanism for the pyrochlore AF\* state. It is also possible that, the magnetic order is induced by the condensation of spinon bilinears in the particle-hole channel from the spinon interaction. The spinon interaction is universally present in the pyrochlore U(1) spin liquid. The more significant ones are the short-range interaction from the exchange interaction. In fact, in Ref. 19, the current authors and collaborators have shown that, the XYZ model already contains a significant spinon interaction. Over there, the spinon interaction was not found to generate an intermediate AF\*-like state between the

U(1) spin liquid and the ordered state. It is, however, still reasonable for us to vision that some other spin exchange may stabilize the pyrochlore AF\* state purely from the spinon interactions.

Despite the possibility of other mechanisms, the pyrochlore AF\* state, once it is realized, should have the expected physical properties. It is these exotic physical properties and the related phenomena that stand out and make the candidate system Nd<sub>2</sub>Sn<sub>2</sub>O<sub>7</sub> exciting.

#### 7. Possibility of the frustrated $\pi$ -flux regime

In this paper, we have chosen the 0-flux for the parent pyrochlore ice U(1) spin liquid. Although the sign of  $J_z$  is ferromagnetic, it is still possible that the rotated transverse coupling can be frustrated. In the case, one would encounter the frustrated  $\pi$  flux U(1) spin liquid. This seems to happen in the Ce-based pyrochlore Ce<sub>2</sub>Sn<sub>2</sub>O<sub>7</sub> and Ce<sub>2</sub>Zr<sub>2</sub>O<sub>7</sub> where the candidate spin liquid was expected to U(1) $\pi$  spin liquid of the octupolar type [27–32].

For the U(1) $\pi$  spin liquid, the spinon realizes the lattice translation symmetry in a projective fashion [16, 51, 52], and the proximate states that grow out of it would naturally break the lattice translation symmetry. For the all-in all-out magnetic order in the Nd-based pyrochlore, the magnetic unit cell is identical to the crystal unit cell, and thus the system preserves the lattice translation. Thus, we do not consider the possibility of the frustrated  $\pi$ -flux regime.

#### 8. Spin-wave theory for “fragmented AFM”

It seems that the other Nd-based dipole-octupole pyrochlore magnets including Nd<sub>2</sub>GaSbO<sub>7</sub>, Nd<sub>2</sub>Zr<sub>2</sub>O<sub>7</sub> and Nd<sub>2</sub>Hf<sub>2</sub>O<sub>7</sub> all develop the all-in all-out magnetic order. Nd<sub>2</sub>Zr<sub>2</sub>O<sub>7</sub> and Nd<sub>2</sub>Hf<sub>2</sub>O<sub>7</sub> are well-interpreted from the picture of moment fragmentation [34, 35, 37, 49]. While these two systems were shown to have the all-in all-out magnetic order, the inelastic neutron scattering pattern at low temperatures develops pinch-point-like structures that are reminiscent of the spin ice, indicating the presence of the spin-ice-like correlation in the spin fluctuations. The “fragmented AFM” in Fig. 1 and Fig. 3 turns to belong to the same phase as the ones that were discussed in Nd<sub>2</sub>Zr<sub>2</sub>O<sub>7</sub> and Nd<sub>2</sub>Hf<sub>2</sub>O<sub>7</sub>. To capture the dynamical property of this phase, it is illuminating to compute the magnetic excitation for the fragmented AFM and compare with the spinon continuum for the U(1) spin liquid and the AF\* state.

As we have remarked, the fragmented AFM develops an experimentally visible order in the  $S^z$  component, and an invisible order in the  $S^x$  component. What is more,  $S^z$  could also function as a disordering operator to quantum mechanically flip the  $S^x$  order and generate the magnetic excitation. That is precisely the reason why one can observe the magnetic excitation with the inelastic neutron scattering measurement.

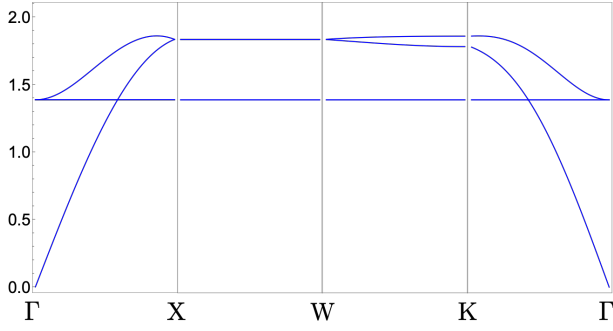


FIG. 5. The spin-wave dispersion along the high symmetry momentum lines for the fragmented AFM state. In the plot, we have set  $\tilde{J}_\perp = 0.6$ , and  $\tilde{J}_x$  is set to unity. Two flat bands are degenerate.

To compute the magnetic excitation, we stay on the horizontal axis of Fig. 1 and consider the model with

$$H = \sum_{\langle ij \rangle} \tilde{J}_x \tilde{S}_i^x \tilde{S}_j^x - \tilde{J}_\perp (\tilde{S}_i^z \tilde{S}_j^z + S_i^y S_j^y). \quad (51)$$

This simplification avoids the complicated crossing coupling between  $\tilde{S}^x$  and  $\tilde{S}^z$  from the second neighbor, but still captures the fragmented nature of the ordering. This Hamiltonian in Eq. (51) has an accidental U(1) symmetry that should be absent in the generic case. For a large  $\tilde{J}_\perp$ , the system develops magnetic order in the  $yz$  plane, and we choose the order to be on the  $\tilde{S}^z$  such that the order is smoothly connected to the generic case with a finite  $J_{2xz}$ . We then perform the spin wave expansion and replace the spin operator with the

Holstein-Primarkoff bosons,

$$\tilde{S}_i^z = \frac{1}{2} - a_i^\dagger a_i, \quad (52)$$

$$\tilde{S}_i^x = \frac{1}{2}(a_i^\dagger + a_i), \quad (53)$$

$$S_i^y = \frac{1}{2i}(a_i - a_i^\dagger), \quad (54)$$

and the Hamiltonian in the linear spin wave theory becomes

$$H = \sum_{\langle ij \rangle} \frac{\tilde{J}_\perp}{2} (a_i^\dagger a_i + a_j^\dagger a_j) + \frac{\tilde{J}_x + \tilde{J}_\perp}{4} (a_i a_j + a_i^\dagger a_j^\dagger) + \frac{\tilde{J}_x - \tilde{J}_\perp}{4} (a_i^\dagger a_j + a_j^\dagger a_i) + const, \quad (55)$$

where the ‘const’ is related to the classical energy and does not influence the magnetic excitation. The magnetic excitations are depicted in Fig. 5. There exist two flat bands that arise from the frustrated interaction in the  $\tilde{S}^x$  component. The spin-ice-like correlation was also argued to be originated from the frustrated  $\tilde{S}^x$  interaction [35]. In Fig. 5, we have a gapless mode at  $\Gamma$  point. This is a Goldstone mode due to the U(1) symmetry breaking of the magnetic order for our model in Eq. (51). In the generic case, we do not have such a continuous symmetry, and we should always expect a gapped spin-wave spectrum.

In the inelastic neutron scattering measurement, only the  $S^z$ - $S^z$  correlation is directly visible. The  $S^z$  operator, under the spin wave expansion, is given as

$$\begin{aligned} S_i^z &= \cos \theta \tilde{S}_i^z + \sin \theta \tilde{S}_i^x \\ &= \cos \theta \left( \frac{1}{2} - a_i^\dagger a_i \right) + \frac{1}{2} \sin \theta (a_i^\dagger + a_i), \end{aligned} \quad (56)$$

where the ordered piece simply contributes to the magnetic Bragg peak, and the second term in Eq. (56) generates the magnetic excitations with single magnons. Moreover, the  $a_i^\dagger a_i$  in Eq. (56) would generate a two-magnon continuum that should appear at high energies that the ones in Fig. 5. This two-magnon continuum might have a very low intensity but seems unavoidable. So far, this two-magnon continuum has not been emphasized in the literature of the Nd-based pyrochlore magnets.